

Supporting Information for

The removal of Cd(II) by the UV/permanaganate process: Role of continuous *in situ* formed MnO₂ and reactive species

Wenrui Wei ^{a,b,1}, Xinwen Kang ^{c,1}, Sining Wu ^a, Virender K. Sharma ^d, Ruijie Xie ^a, Beicheng Xia ^a,

Kaiheng Guo ^{a,*}, Jingyun Fang ^a

^a Guangdong Provincial Key Laboratory of Environmental Pollution Control and Remediation Technology, School of Environmental Science and Engineering, Sun Yat–Sen University, Guangzhou 510275, China

^b Guangzhou Environmental Protection Investment Group Co., Ltd., Guangzhou 510170, China

^c Chengdu Academy of Environmental Sciences, Chengdu 610072, China

^d Department of Environmental and Occupational Health, School of Public Health, Texas A&M University, College Station, Texas 77843, United States

* Corresponding author, phone: +86–15692415065; e–mail: guokh3@mail.sysu.edu.cn.

¹ Shared the first authorship

Submitted to:

Environmental Science: Water Research & Technology

Number of pages (including this page): 17

Number of Text: 1

Number of Figures: 14

List of captions:

Text S1. Calculation method of concentration of KMnO_4 and in situ formed MnO_2 .	3
Figure S1. pH variation during Cd(II) removal by the UV/permanganate process at pH_0 6.0. Conditions: $[\text{KMnO}_4]_0 = 100 \mu\text{M}$, $[\text{Cd(II)}]_0 = 20 \mu\text{M}$.	4
Figure S2. Distribution of Cd(II) species with pH variation.	5
Figure S3. Time-dependent formation of MnO_2 during the Cd(II) removal by the UV/permanganate process at pH_0 6.0. Conditions: $[\text{KMnO}_4]_0 = 100 \mu\text{M}$, $[\text{Cd(II)}]_0 = 20 \mu\text{M}$.	6
Figure S4. Time-dependent UV-vis spectra at the wavelengths of 200 - 800 nm in the UV/permanganate process with a permanganate dosage of 100 μM (a) in the absence of PP and (b) in the presence of 5 mM PP.	7
Figure S5. (a) The effects of PP on Cd(II) removal by prepared MnO_2 . Conditions: $\text{pH} = 6.0$, $[\text{MnO}_2]_0 = 65 \mu\text{M}$, $[\text{Cd(II)}]_0 = 20 \mu\text{M}$, $[\text{PP}] = 5 \text{ mM}$. (b) UV-vis spectra at the wavelengths of 200 - 800 nm of MnO_2 in the absence/presence of 5 mM PP. Conditions: $\text{pH} = 6.0$, $[\text{MnO}_2]_0 = 65 \mu\text{M}$, $[\text{Cd(II)}]_0 = 20 \mu\text{M}$, $[\text{PP}] = 5 \text{ mM}$.	8
Figure S6. The kinetics of Cd(II) removal by the MnO_2 /permanganate and UV/ MnO_2 process. Conditions: $\text{pH}_0 = 6.0$ and 8.0, $[\text{MnO}_2]_0 = [\text{KMnO}_4]_0 = 65 \mu\text{M}$, $[\text{Cd(II)}]_0 = 20 \mu\text{M}$.	9
Figure S7. (a) Adsorption isotherm of Cd(II) onto MnO_2 . Conditions: $\text{pH}_0 = 6.0$, $[\text{MnO}_2]_0 = 100 \mu\text{M}$, $[\text{Cd(II)}]_0 = 1 - 100 \mu\text{M}$. XPS spectra of (b) Cd 3d _{5/2} , (c) O 1s of MnO_2 adsorbed Cd(II) matching Langmuir fit curves. Conditions: $\text{pH}_0 = 6.0$, $[\text{MnO}_2]_0 = 100 \mu\text{M}$, $[\text{Cd(II)}]_0 = 2 \mu\text{M}$. (d) O 1s spectra of MnO_2 generated in UV/permanganate process without Cd(II). Conditions: $\text{pH}_0 = 6.0$, $[\text{MnO}_2]_0 = 100 \mu\text{M}$. XPS spectra of (e) Cd 3d _{5/2} , (f) O 1s of MnO_2 adsorbed Cd(II) matching linear fit curves. Conditions: $\text{pH}_0 = 6.0$, $[\text{MnO}_2]_0 = 100 \mu\text{M}$, $[\text{Cd(II)}]_0 = 100 \mu\text{M}$.	10
Figure S8. Removal rate of Cd(II) by the (a) UV irradiation and (b) permanganate at pH_0 5.0 - 7.0. Conditions: $[\text{KMnO}_4]_0 = 100 \mu\text{M}$, $[\text{Cd(II)}]_0 = 20 \mu\text{M}$.	11
Figure S9. Effect of pH_0 on MnO_2 generation in the UV/permanganate process during Cd(II) removal. Conditions: $\text{pH}_0 = 5.0 - 7.0$, $[\text{KMnO}_4]_0 = 100 \mu\text{M}$, $[\text{Cd(II)}]_0 = 20 \mu\text{M}$.	12
Figure S10. pH variation during Cd(II) removal by the (a) UV/permanganate process, (b) UV irradiation and (c) permanganate at pH_0 5.0 - 7.0. Conditions: $[\text{KMnO}_4]_0 = 100 \mu\text{M}$, $[\text{Cd(II)}]_0 = 20 \mu\text{M}$.	13
Figure S11. pH variation during Cd(II) removal by the UV/permanganate process in the presence of cations. Conditions: $[\text{KMnO}_4]_0 = 100 \mu\text{M}$, $[\text{Cd(II)}]_0 = 20 \mu\text{M}$, $[\text{Ca(II)}]_0 = [\text{Mg(II)}]_0 = 1 \text{ mM}$, $\text{pH}_0 = 6.0$.	14
Figure S12. SEM-EDS of MnO_2 generated from UV/permanganate process during Cd(II) removal in the presence of (a) Ca(II) and (b) Mg(II). Conditions: $[\text{KMnO}_4]_0 = 100 \mu\text{M}$, $[\text{Cd(II)}]_0 = 20 \mu\text{M}$, $[\text{Ca(II)}]_0 = [\text{Mg(II)}]_0 = 1 \text{ mM}$.	15
Figure S13. pH variation during Cd(II) removal by the UV/permanganate process in the presence of NOM. Conditions: $[\text{KMnO}_4]_0 = 100 \mu\text{M}$, $[\text{Cd(II)}]_0 = 20 \mu\text{M}$, $[\text{NOM}]_0 = 3 \text{ mg/L}$.	16
Figure S14. (a) The final testing solution of Cd(II) removal by the UV/ KMnO_4 process in tap water for 1 h. (b) The time-dependent concentration of colloidal MnO_2 during Cd(II) removal by UV/ KMnO_4 in tap water. Conditions: $[\text{KMnO}_4]_0 = 100 \mu\text{M}$, $[\text{Cd(II)}]_0 = 20 \mu\text{M}$, $\text{pH}_0 = 6.0$.	17

Text S1. Calculation method of concentration of KMnO_4 and in situ formed MnO_2 .

KMnO_4 concentration can be determined by UV/vis spectrophotometry (TU-1900, Persee Co., China) at 418 and 525 nm simultaneously by Equation S4 derived from Equations S1 - S3, while MnO_2 was determined at 418 nm. Note that permanganate shows negligible absorbance at 418 nm.

$$A_t^{525} = [\text{Mn(VII)}]_t \epsilon_{\text{KMnO}_4}^{525} + [\text{MnO}_2]_t \epsilon_{\text{MnO}_2}^{525} \quad (\text{S1})$$

$$[\text{Mn(VII)}]_t = (A_t^{525} - \epsilon_{\text{MnO}_2}^{525} [\text{MnO}_2]_t) / \epsilon_{\text{KMnO}_4}^{525} \quad (\text{S2})$$

$$[\text{Mn(VII)}]_t = (A_t^{525} - \epsilon_{\text{MnO}_2}^{525} A_t^{418} / \epsilon_{\text{MnO}_2}^{418}) / (A_0^{525} / [\text{Mn(VII)}]_0) \quad (\text{S3})$$

$$[\text{Mn(VII)}]_t = (A_t^{525} - A_f^{525} A_t^{418} / A_f^{418}) / (A_0^{525} / [\text{Mn(VII)}]_0) \quad (\text{S4})$$

where A means the absorbance, the superscript means wavelength, and the sub-scripts 0, f, and t represent initial, final, and variable time. In this study, the KMnO_4 was irradiated by ultra-violet for 3 hours to completely transform to MnO_2 colloids and then immediately measure the final absorbance.

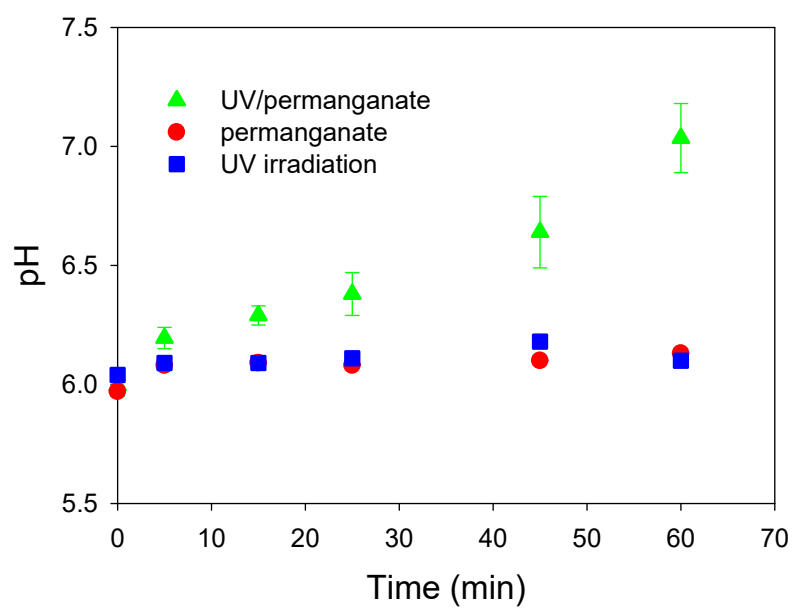


Figure S1. pH variation during Cd(II) removal by the UV/permanganate process at pH₀ 6.0.

Conditions: [KMnO₄]₀ = 100 μM, [Cd(II)]₀ = 20 μM.

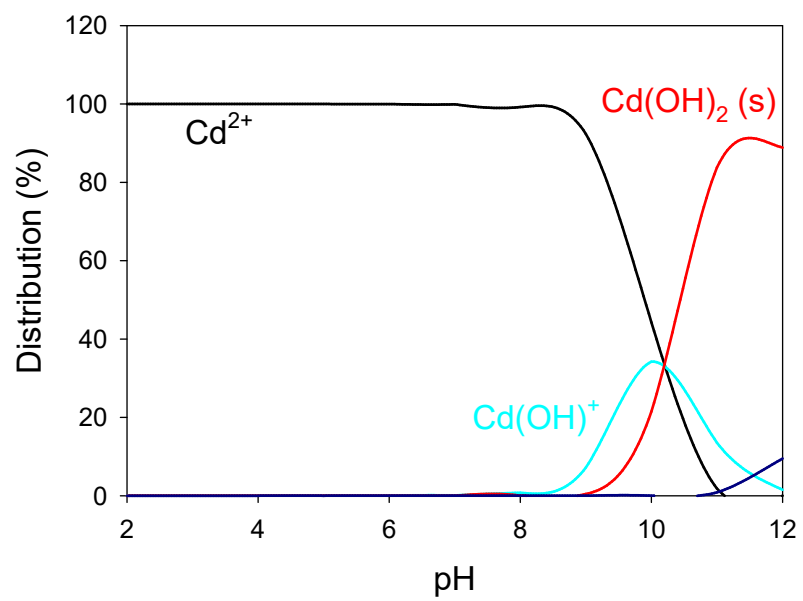


Figure S2. Distribution of Cd(II) species with pH variation.

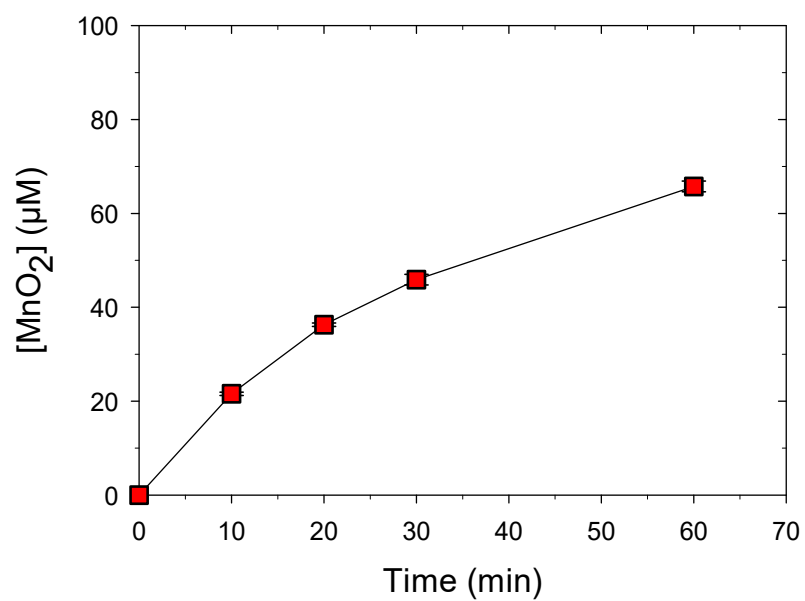


Figure S3. Time-dependent formation of MnO₂ during the Cd(II) removal by the UV/permanganate process at pH₀ 6.0. Conditions: [KMnO₄]₀ = 100 μM, [Cd(II)]₀ = 20 μM.

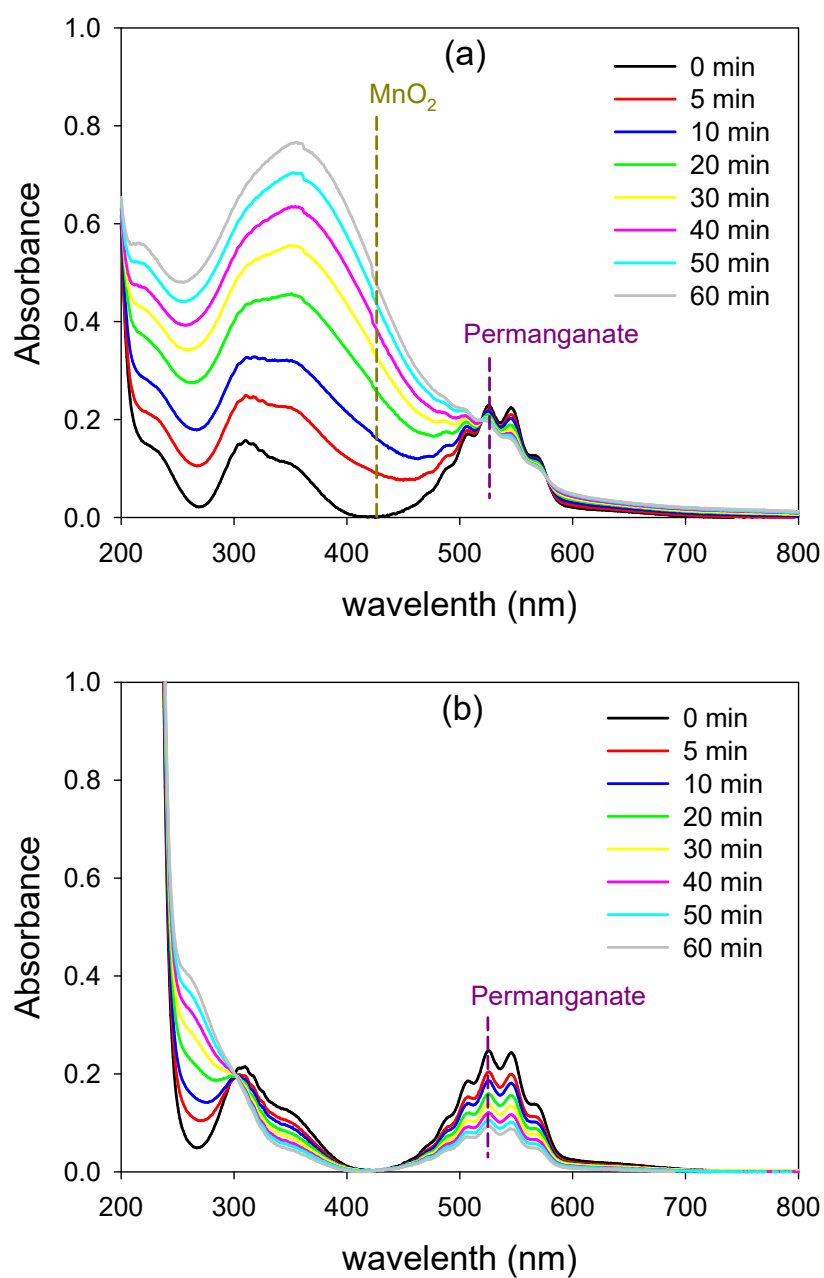


Figure S4. Time-dependent UV-vis spectra at the wavelengths of 200 - 800 nm in the UV/permanganate process with a permanganate dosage of 100 μM (a) in the absence of PP and (b) in the presence of 5 mM PP.

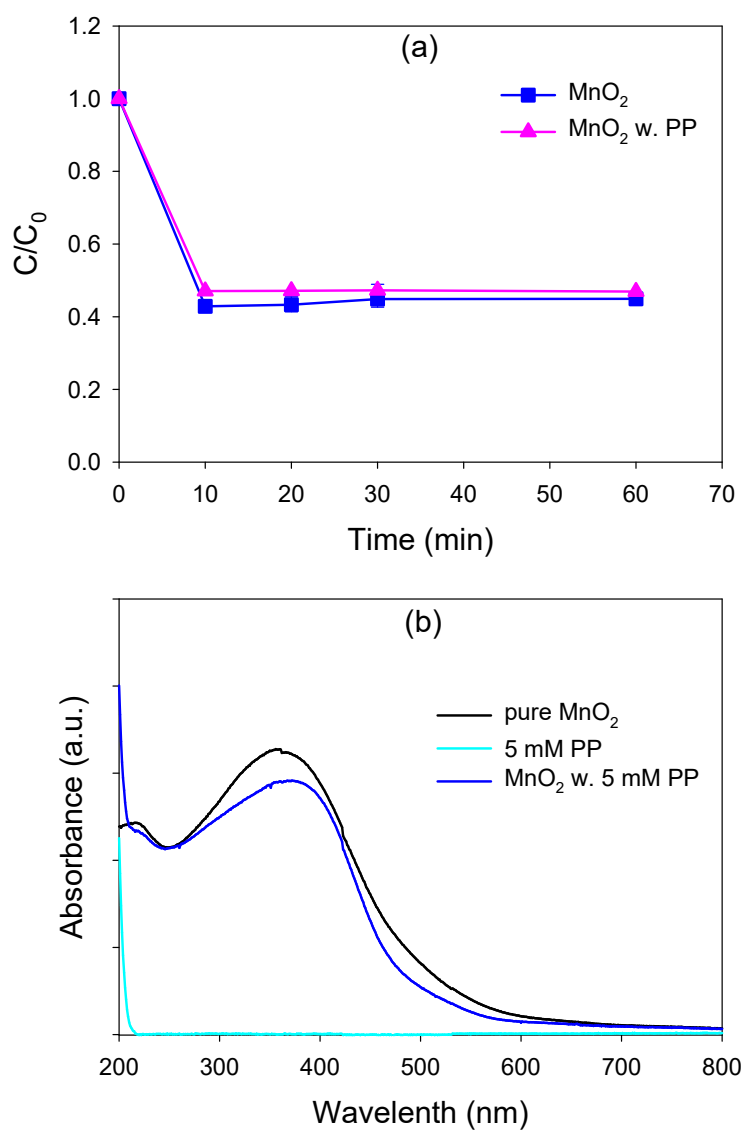


Figure S5. (a) The effects of PP on Cd(II) removal by prepared MnO_2 . Conditions: pH = 6.0, $[MnO_2]_0 = 65 \mu M$, $[Cd(II)]_0 = 20 \mu M$, $[PP] = 5 \text{ mM}$. (b) UV-vis spectra at the wavelengths of 200 - 800 nm of MnO_2 in the absence/presence of 5 mM PP. Conditions: pH = 6.0, $[MnO_2]_0 = 65 \mu M$, $[Cd(II)]_0 = 20 \mu M$, $[PP] = 5 \text{ mM}$.

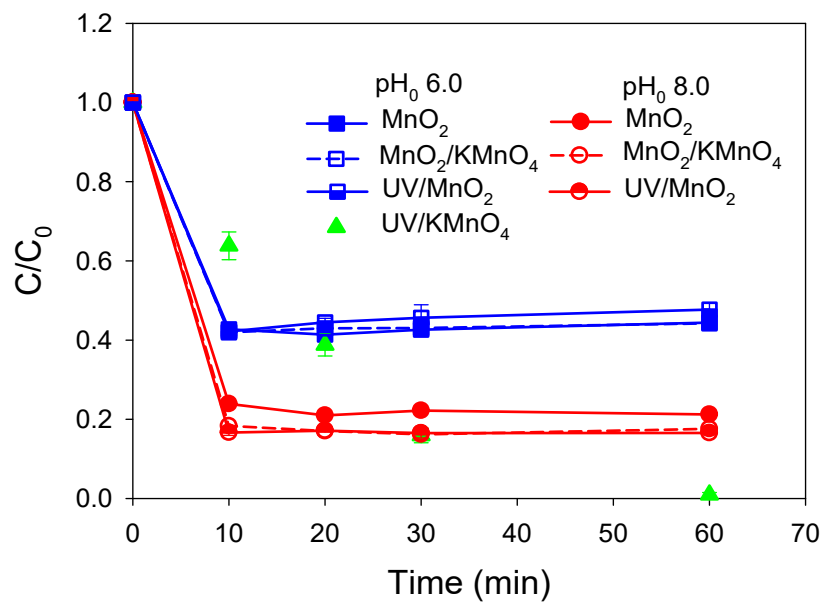


Figure S6. The kinetics of Cd(II) removal by the MnO₂/permanganate and UV/MnO₂ process.

Conditions: pH₀ = 6.0 and 8.0, [MnO₂]₀ = [KMnO₄]₀ = 65 μM, [Cd(II)]₀ = 20 μM.

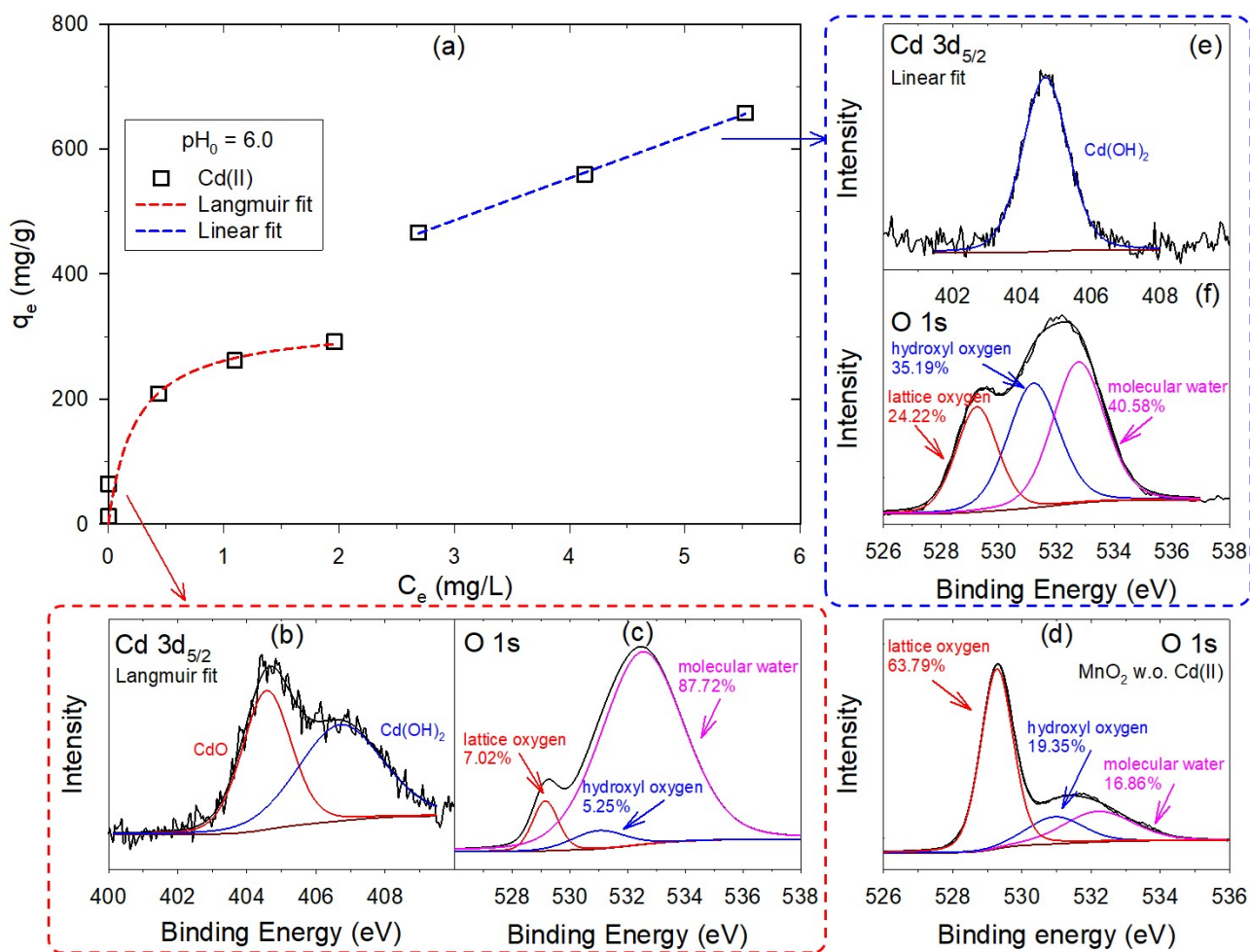


Figure S7. (a) Adsorption isotherm of Cd(II) onto MnO₂. Conditions: pH₀ = 6.0, [MnO₂]₀ = 100 μM, [Cd(II)]₀ = 1 - 100 μM. XPS spectra of (b) Cd 3d_{5/2}, (c) O 1s of MnO₂ adsorbed Cd(II) matching Langmuir fit curves. Conditions: pH₀ = 6.0, [MnO₂]₀ = 100 μM, [Cd(II)]₀ = 2 μM. (d) O 1s spectra of MnO₂ generated in UV/permanaganate process without Cd(II). Conditions: pH₀ = 6.0, [MnO₂]₀ = 100 μM. XPS spectra of (e) Cd 3d_{5/2}, (f) O 1s of MnO₂ adsorbed Cd(II) matching linear fit curves. Conditions: pH₀ = 6.0, [MnO₂]₀ = 100 μM, [Cd(II)]₀ = 100 μM.

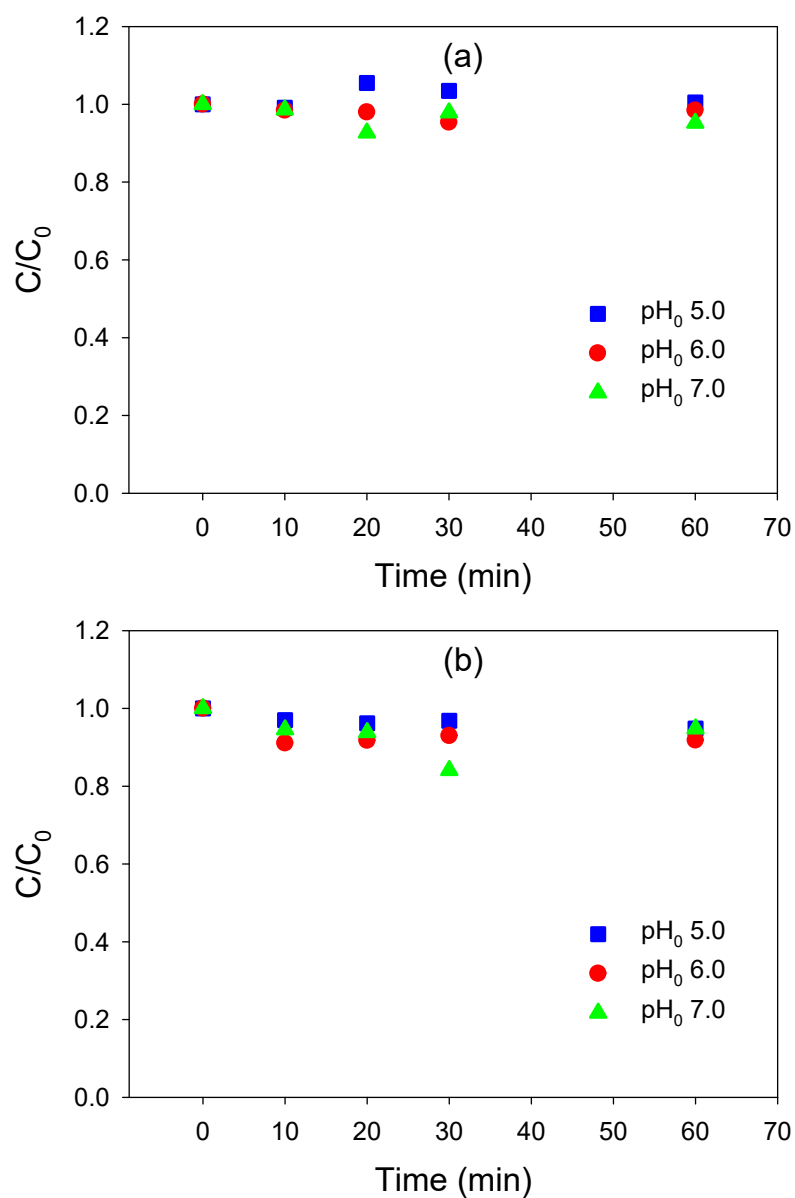


Figure S8. Removal rate of Cd(II) by the (a) UV irradiation and (b) permanganate at pH_0 5.0 - 7.0.

Conditions: $[\text{KMnO}_4]_0 = 100 \mu\text{M}$, $[\text{Cd(II)}]_0 = 20 \mu\text{M}$.

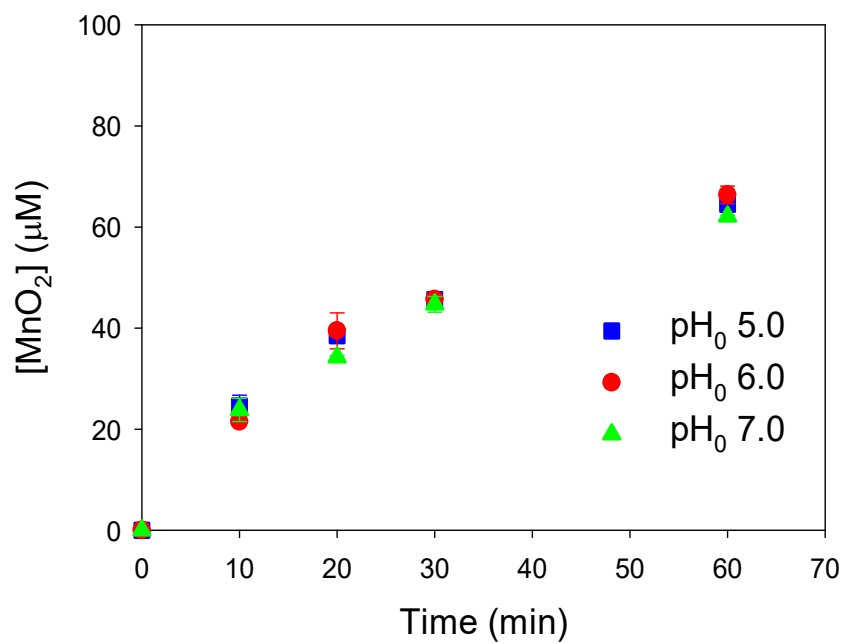


Figure S9. Effect of pH₀ on MnO₂ generation in the UV/permanganate process during Cd(II) removal.

Conditions: pH₀ = 5.0 - 7.0, [KMnO₄]₀ = 100 µM, [Cd(II)]₀ = 20 µM.

Figure S10. pH variation during Cd(II) removal by the (a) UV/permanganate process, (b) UV irradiation and (c) permanganate at pH₀ 5.0 - 7.0. Conditions: [KMnO₄]₀ = 100 μM, [Cd(II)]₀ = 20 μM.

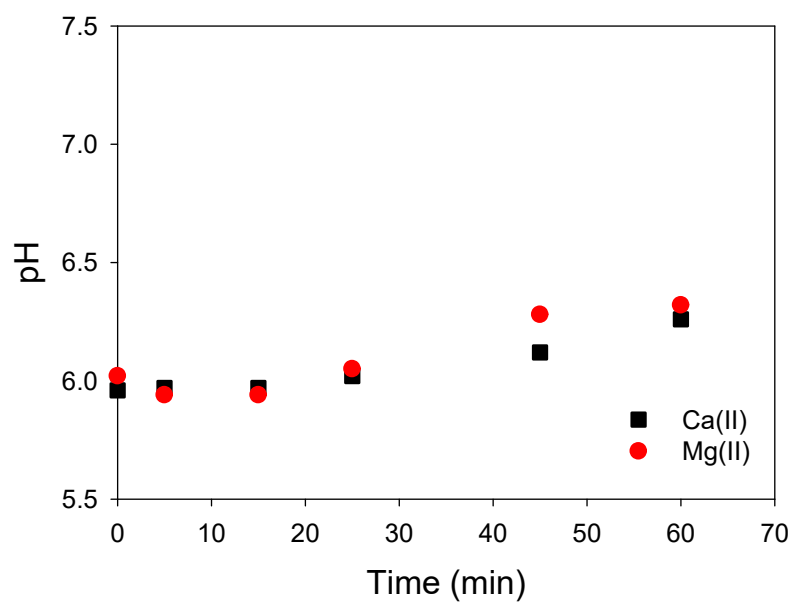


Figure S11. pH variation during Cd(II) removal by the UV/permanganate process in the presence of cations. Conditions: $[\text{KMnO}_4]_0 = 100 \mu\text{M}$, $[\text{Cd(II)}]_0 = 20 \mu\text{M}$, $[\text{Ca(II)}]_0 = [\text{Mg(II)}]_0 = 1 \text{ mM}$, $\text{pH}_0 = 6.0$.

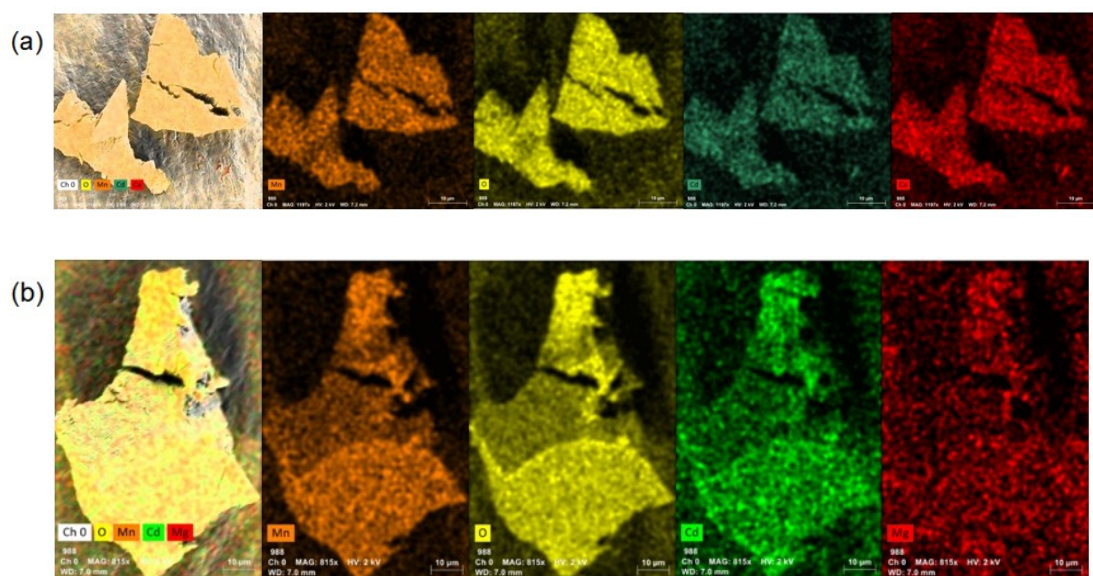


Figure S12. SEM-EDS of MnO_2 generated from UV/permanaganate process during Cd(II) removal in the presence of (a) Ca(II) and (b) Mg(II) . Conditions: $[\text{KMnO}_4]_0 = 100 \mu\text{M}$, $[\text{Cd(II)}]_0 = 20 \mu\text{M}$, $[\text{Ca(II)}]_0 = [\text{Mg(II)}]_0 = 1 \text{ mM}$.

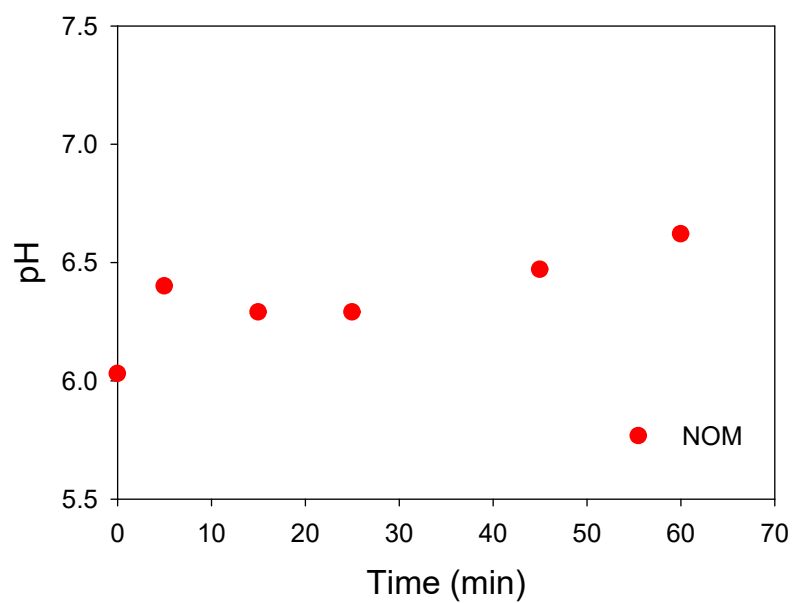


Figure S13. pH variation during Cd(II) removal by the UV/permanganate process in the presence of NOM. Conditions: $[\text{KMnO}_4]_0 = 100 \mu\text{M}$, $[\text{Cd(II)}]_0 = 20 \mu\text{M}$, $[\text{NOM}]_0 = 3 \text{ mg/L}$.

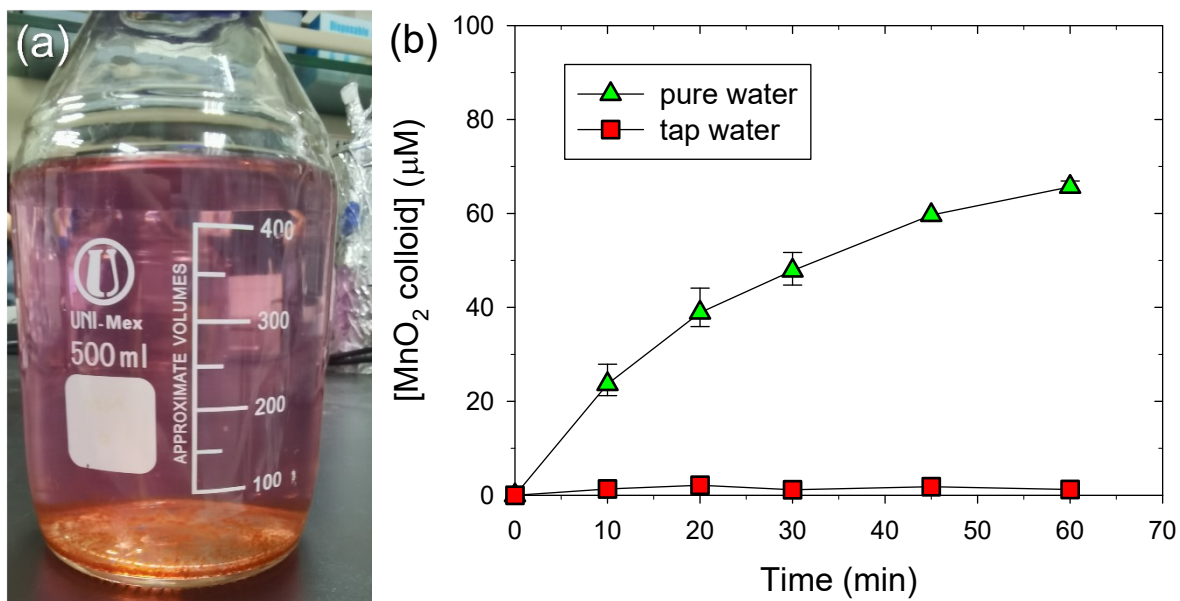


Figure S14. (a) The final testing solution of Cd(II) removal by the UV/ KMnO_4 process in tap water for 1 h. (b) The time-dependent concentration of colloidal MnO_2 during Cd(II) removal by UV/ KMnO_4 in tap water. Conditions: $[\text{KMnO}_4]_0 = 100 \mu\text{M}$, $[\text{Cd(II)}]_0 = 20 \mu\text{M}$, $\text{pH}_0 = 6.0$.